



Characterization of TiO₂ Photoanode and Dye Sensitized Photoanode for DSSC Applications

S Vedavarshni, T Raguram and K S Rajni*

Department of Sciences, Amrita Vishwa Vidyapeetham, Coimbatore – 641 112, India

*ks_rajani@cb.amrita.edu

Abstract: In the present work a simple sol-gel technology employing acetic acid as hydrolyzing agent (HA) is illustrated for preparing TiO₂ Nanoparticles for its suitability as Photoanode in DSSC's. The electrode composed of ~9nm spherical anatase nanocrystallites of Titania, showed 95% optical transmittance with 3.05eV bandgap. Sensitization of the photoanode is also emphasized for better understanding of characteristics for improving oxide based semiconducting Dye Sensitized Solar Cells (DSSC's). The ethanol extracts of Tecoma Stans is the sensitizer here showing maximum absorption around 650nm with ~2eV bandgap. FTIR analysis of the prepared anode and sensitizer includes similar functional groups which justifies better lattice matching between them thus Photoanode degradation of natural sensitizer is addressed to an extent thus owing to better photovoltaic performan.

Keywords: Sol-gel, XRD, FESEM, Natural sensitizer, DSSC.

I. INTRODUCTION

The Dye-sensitized solar cell (DSSC), the promising new generation solar energy technology is given importance due to its high transfer efficiency, low cost and easy preparation process [1,2] as reported by Gratzel and coworkers in 1991 [1]. It involves a prototype realizing the optical absorption by a sensitization and charge separation process by a wide band gap semiconductor with nanocrystalline morphology [1]. TiO₂ being the best choice of photoanode due to its recombination probabilities and electronic configuration. It exists in three phases Anatase, Rutile and Brookite among which anatase (~3.0eV) acts as a good window material in photovoltaic applications. The preparation of controlled TiO₂ morphologies at various sizes and phases implies on the synthesis route and experimental conditions such as TiO₂ precursor, surfactant, solvent effect, temperature and duration of the process. [3-7].

Sensitization of nanoporous TiO₂ enhances the collection of low energy photons and thus extend the spectral sensitivity of the Photoanode. Due to the high cost, difficult synthesis procedure and environmental issues due to metal complexes involved, limited the wide range applications of inorganic, synthetic dyes. In this regard, the non-toxic, biodegradable and cost effective natural dyes have been the subject of study in sensitizer research.

In the present work TiO₂ electrodes are prepared by sol-gel technique together with doctor blade method [8]. Also as-prepared oxide gel is amorphous and by subsequent thermal

treatment at suitable temperatures, crystalline TiO₂ films are produced. The natural ethanol extract of Tecoma Stans flower is used as sensitizer. The structural, morphological and optical analysis are investigated for photoanode and phytochemical analysis, structural and optical analysis are carried out for sensitizer. Also the compatibility of both components are also analyzed towards better cell performance.

II. EXPERIMENTAL

A. TiO₂ Nanoparticles Synthesis and Characterisation

TiO₂ nanocrystallites are synthesized by Sol-Gel method with acetic acid as the hydrolyzing agent. The sample after coated onto the FTO substrate, taken for calcination at 400°C for about 30 minutes.

Structural analysis is carried out by Powder X-ray diffraction analysis using Shimadzu XRD 6000 diffractometer with CuK α radiation (λ = 1.541 Å). The functional group of the prepared sample is confirmed by FTIR

From a field emission scanning electron microscope (FESEM) using FEGQUANTA 250 combined with an energy dispersive spectroscopy (EDS), the composition and surface morphology is studied. The luminescence studies using RF 6000 and the reflectance UV-DRS study is taken in the region of 200 to 800nm.



In The extraction of phytochemicals of Tecoma Stans is done at room temperature by soaking the flowers in ethanol.

Phytochemical screening test is carried out for the dye extract using the standard method [9] as in table1to identify the presence of active functional structures. The pigment was also subjected to absorption studies and FTIR.

PHYTOCHEMICAL	TEST	INDICATOR
PHENOL	1 ml of extract + 2 ml of distilled water + 10% FeCl ₃	Blue or green color
ANTHOCYANIN	a) Extract + 10% NaOH b) Extract + conc.H ₂ SO ₄ c) Small amount of extract + 2N NaOH	a) Blue color b) Yellowish orange c) Blue-green color
QUINONES	1 ml of extract + 1 ml conc.H ₂ SO ₄	Red color
CUOMARINES	1 ml of extract + 1 ml of 10% NaOH	Yellow color
ANTHRAQUINONE S	1 ml of extract + few drops of 10% NaOH	Pink color precipitate
FLAVONOIDS	a) 1 ml extract + few drops of NaOH b) 1 ml extract + few drops of NaOH + few drops of dilute acid	a) An intense yellow color b) Colorless appearance

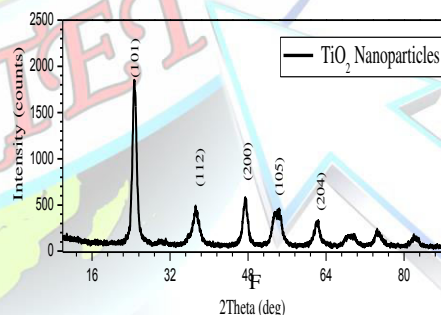
calculated using Eq.

$$1/d^2_{hkl} = [(h^2 + k^2)/a^2] + [l^2/c^2] \text{ -----(1)}$$

(Where, dhkl is the spacing between the planes corresponding to Miller indices (hkl)), the calculated lattice constant, a= 3.83 Å⁰ and c= 9.49 Å⁰ matches with the standard data for anatase TiO₂ (JCPDS Card No 21-1272). The average crystallite size of the most prominent anatase (101) was calculated using Sherrer formula [10], is given by Eq. (2)

$$D = K \lambda / \beta \cos \theta \text{ ----- (2)}$$

(Where λ the X-ray wavelength of the CuKα radiation (1.541Å⁰), β the full width at half maximum (FWHM) in radian and θ is the Bragg's diffraction angle). The average crystallite size is found to be around 9 nm which is less than the commercial available TiO₂ nanoparticles (20nm).The surface morphology(Fig. 1b)) FESEM shows uniformly distributed spherical sized particles which is attributed to the hydrolyzing agent [11]. Also the spatial confinement of mesopores array controls the formation and growth of anatase phase thereby leading to a more or less uniform distribution of Titania nanocrystals [12], which enhances the conversion of the amorphous film into anatase - phase

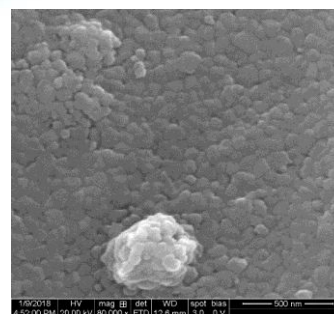
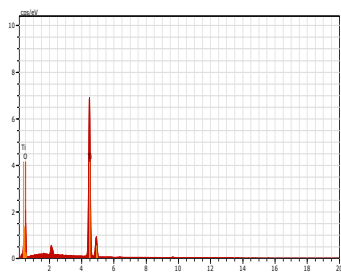


a)

III. RESULTS AND DISCUSSIONS

A. Characterisation of Photoanode

The observed diffraction peaks (Fig.1a)) corresponding to the planes (101), (112), (200), (105) and (204) confirms the tetragonal anatase phase of TiO₂ (JCPDS Card No 21-1272). Microstructural parameters calculated for the most prominent peak (101) in Table 2. constants (a and c) for planes structure





showed indirect transition and the optical band gap 3.0eV [15-17].

b)

Fig. 1: a) XRD patterns of synthesized TiO_2 nanocrystallites. b) FESEM and EDS images of TiO_2 thin film

TABLE 2: MICROSTRUCTURAL ANALYSIS OF SYNTHESIZED TiO_2 NANOCRYSTALLITES

Sample	TiO_2 Nanoparticles
(hkl)	(101)
FWHM	0.98
Lattice Constant(\AA) a	3.83
c	9.49
Crystallite Size (D) nm	9
Strain 10^{-3}	4.15
Dislocation Density 10^{16} lines m^{-2}	1.31

B. Functional Group Analysis

In From Fig. 2, the broad band around $3000 - 3500 \text{ cm}^{-1}$ corresponds to stretching vibrations OH of hydroxyl groups which is probably due to the fact that the spectra were recorded in situ and some reabsorptions of water from the ambient atmosphere has occurred [13]. The peak at 440 cm^{-1} corresponds to O-Ti-O vibration which is the characteristics of TiO_2 lattice. The peak observed at 2926 cm^{-1} , 2853 cm^{-1} and 1615 cm^{-1} corresponds to H-OH stretching, CH stretching and hydroxyl(bending) groups such as C=C stretching group of molecular water [14] respectively.

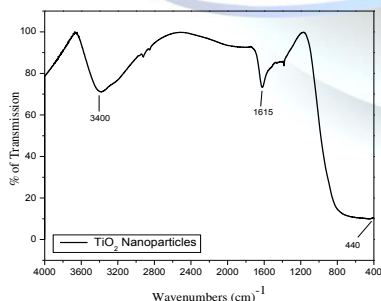
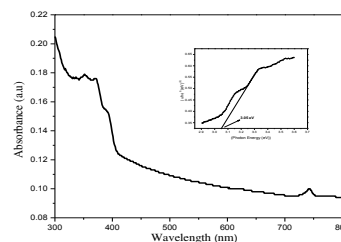


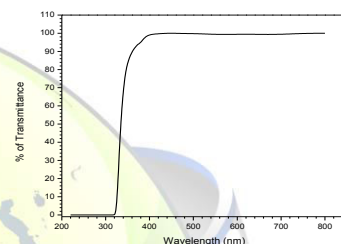
Fig. 2: FTIR spectra synthesized of TiO_2 nanocrystallites

C. Optical Analysis

Fig 3a) it is seen that the optical absorption is between 300-400nm and 700-800nm. From Fig. 3b) it is summarized that % transmittance is $\sim 95\%$, Tauc plot of $(\alpha h\nu)^{1/2}$ vs. $h\nu$



a)



b)

Fig. 3: a) UV-VIS absorption and bandgap of prepared TiO_2 nanocrystallites. b) % Transmittance TiO_2 thin film

D. Photoluminescence

Photoluminescence (PL) emission spectra recorded with excitation wavelength at 400 nm showed strong band around 384 which is due to the transition of electrons from conduction band to valence band, the energy gap of TiO_2 [18]. A broad blue emission found around $400 - 500 \text{ nm}$ is due to oxygen vacancy in TiO_2 film [19, 20].

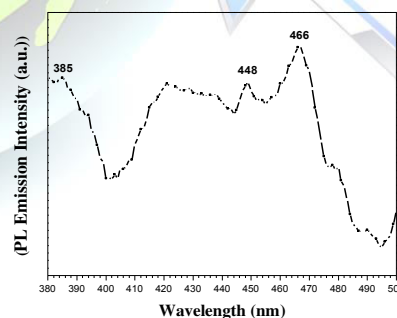


Fig. 4: Photoluminescence spectra of the TiO_2 thin film

E. Characterization of sensitizer:-Phytochemical analysis

The Phytochemical analysis of the flower extract confirmed the presence of structures such as phenols, anthocyanin and flavonoids which are responsible for the dye absorption.



F. Dye Stability

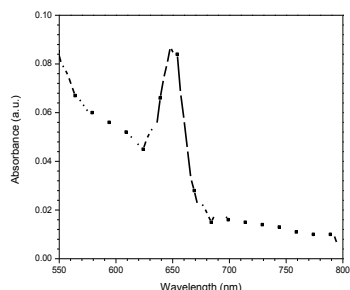


Fig. 5: UV-Visible spectra of Tecoma Stans dye

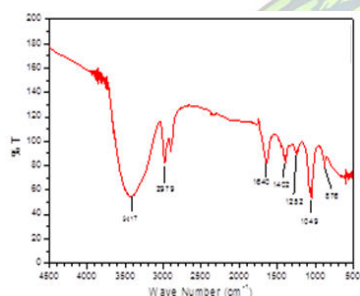


Fig. 6: FTIR spectra of Tecoma stans

The prepared dye when subjected to UV-Visible irradiation (Fig 4), showed absorption around 650nm and bandgap was found to be 2eV. The FTIR analysis (Fig 5) has also got similar functional groups as that of prepared TiO₂ thin film (Fig 2) owing to better lattice matching and less degradation by TiO₂ over a period of time due to consistent UV irradiance.

IV. CONCLUSION

Using acetic acid as hydrolyzing agent has influenced the co-precipitation part of the sol-gel method which has increases the crystallinity of the TiO₂ nanocrystallites to about 9nm crystallite size which is much lesser than commercial available one (20nm). Morphological analysis shows the spherical shape of the nanoparticles with almost uniform distribution due to the space confinement induced by the HA during synthesis. Optical analysis shows 95 % of transmission. The observed blue emission around 400 to 500nm in the PL spectrum is due to oxygen vacancy and the band observed around 385nm is due to the transition of electrons from conduction band to valence band. The Tecoma extract showed absorption around 550nm. Also from FTIR analysis similarity of the extracted dye lattice

with that of the thin film prepared was observed. Thus this dye could be more stable than any other conventional natural extract used as sensitizer so far. From the results it is concluded that nanocrystallites prepared exhibited the optimal structural properties with pure anatase phase, crystallite size and PL intensity. In addition using the Tecoma extract pi as sensitizer it is expected to improve the active region of the synthesized TiO₂ Photoanode as it has better lattice compatibility probing to better efficiency for DSSC if commercialized.

REFERENCES

- [1] K. Brian O'Regan, Michael Grätzel, "A low cost, highefficiency solar cell based on dye-sensitized colloidal TiO₂ films", *Nature*, vol. 335, pp. 737, (1991).
- [2] Qifeng Zhang, Guozhong Cao, Nanostructured photoelectrodes for dye-sensitized solar cells, *NanoToday*, vol. 6, pp. 91-109, 2011.
- [3] H.-Y. Chen, D.-B. Kuang, C.-Y. Su, "Hierarchically micro/nanostructured photoanode materials for dye-sensitized solar cells", *J. Mater. Chem.*, vol. 22, pp. 15475-15489, 2012.
- [4] M. Pal, J. García Serrano, P. Santiago, U. Pal, "Size-Controlled Synthesis of Spherical TiO₂ Nanoparticles: Morphology, Crystallization, and Phase Transition", *J. Phys. Chem. C*, vol. 111, pp. 96-102, 2007.
- [5] S.J. Kwon, H.B. Im, J.E. Nam, J.K. Kang, T.S. Hwang, K.B. Yi, "Hydrothermal synthesis of rutile-anatase TiO₂ nanobranched arrays for efficient dye-sensitized solar cells", *Appl. Surf. Sci.*, vol. 320, pp. 487-493, 2014.
- [6] S. Kathirvel, C. Su, H.-C. Lin, B.-R. Chen, W.-R. Li, "Facile non-hydrolytic solvothermal synthesis of one dimensional TiO₂ nanorods for efficient dye-sensitized solar cells", *Mater. Lett.*, vol. 129, pp. 149-152, 2014.
- [7] L. De Marco, M. Manca, R. Buonsanti, R. Giannuzzi, F. Malara, P. Pareo, L. Martiradonna, N.M. Giancaspro, P.D. Cozzoli, G. Gigli, "High-quality photoelectrodes based on shape-tailored TiO₂ nanocrystals for dye-sensitized solar cells", *J. Mater. Chem.*, vol. , pp. 13371-13379, 2011.
- [8] J.D. Mackenzie, "Applications of the Sol-Gel Process", *J. Non-Cryst. Solids*, vol. 48, pp.48, 1982.
- [9] G. Anburaj, M. Marimuthu, V. Rajasudha and Dr. R Manikandan, "Phytochemical screening and GC-MS analysis of ethanolic extract of Tecoma stans (Family: Bignoniaceae) Yellow Bell Flowers", *Journal of Pharmacognosy and Phytochemistry*, vol. 5, pp. 172-175, 2016.
- [10] F.B. Moges Tsegaa, Dejene, "Influence of acidic pH on the formulation of TiO₂ nanocrystalline powders with enhanced photoluminescence property", *Heliyon* vol. 3, pp. e00246, 2017.
- [11] Wenxiu Que, A.Uddin, X.Hu, "Thin film TiO₂ electrodes derived by Sol-gel process for photovoltaic applications", *Journal of power sources*, vol. 159, pp. 353-356, 2006.
- [12] A.L.Patterson, "The Scherrer formula for X-ray particle size determination", *Phys. Rev.*, vol.56, pp. 978-982, 1939.
- [13] A.N JoseA, J.T. Juan, D. Pablo, R.P. Javier, R. Diana, I.L. Marta, *Appl. Catal., A Gen.* vol. 178, pp. 91, 1999.
- [14] Y. Zhao, C. Li, X. Liu, F. Gu, H. Jiang, W. Shao, L. Zhang, Y. He, "Synthesis and optical properties of TiO₂ nanoparticles", *Mater. Letter.*, vol. 61, pp. 79-83, 2007.
- [15] A.S Bakri1, M.Z Sahdan1, F Adriyanto1, N.A. Raship, N.D.M Said, S.A Abdullah and M.S Rahim, "Effect of Annealing Temperature of



International Journal of Advanced Research Trends in Engineering and Technology (IJARTET)
Vol. 5, Special Issue 12, April 2018

- Titanium Dioxide Thin Films on Structural and Electrical Properties”, AIP Conference Proceedings, vol. 1788, pp. 030030, 2017.
- [16] N.Gokilamani, N.Muthukumarasamy, M.Thambidurai, “Synthesis and characterization of nanocrystalline TiO₂ thin films by solgel dip coating method”, Advanced Materials Research, Vol. 678, pp. 108-112, 2013.
- [17] R.S. Dubey, “Temperature-dependent phase transformation of TiO₂ nanoparticles synthesized by sol-gel method”, Materials letters, vol. 215, pp. 312-317, 2018.
- [18] T.S. Senthil, N. Muthukumarasamy, S. Agilan, , M. Thambidurai, R. Balasundaraprabhu, “Preparation and characterization of nanocrystalline TiO₂ thin films”, Materials Science and Engineering B, vol. 174, pp. 102-104, 2010.
- [19] Y.-H. Chang, C.-M. Liu, C. Chen, H.-E. Cheng, “The effect of geometric structure on photoluminescence characteristics of 1-D TiO₂ nanotubes and 2D TiO₂ films fabricated by atomic layer deposition”, J.Electrochem. Soc., vol. 159, pp. D401-D405, 2012.
- [20] B. Choudhury and A. Choudhury, “Low-Dimensional Systems and Nanostructures”, Physica E, vol. 56, pp. 364–371, 2014..

